



ISSN: 0067-2904

Effect of Voltage on Gas Sensor Performance of Anodization Synthesized TiO₂ Nanotubes Arrays

Mina Mohammed Faris¹, Asmaa Kadim Ayal^{2*}

¹Department of Chemistry, College of Science, University of Baghdad, 10071 Baghdad, Iraq

²Department of Chemistry, College of Science for Women, University of Baghdad, 10071 Baghdad, Iraq

Received: 18/12/2022 Accepted: 3/3/2023 Published: 30/12/2023

Abstract

Serious gases have been highly related to being prejudiced against human life within the environment. The evolution of a trustworthy gas sensor with an elevated response is of major importance for detecting various hazardous gases. Titanium dioxide (TiO₂) nanotubes (TNTs) are favorable candidates with considerable potential and stellar performance in gas sensor applications. In this work, we have studied the effect of voltage on preparing TiO₂ nanotubular arrays via the anodization technique for gas sensor applications. A simple electrochemical anodization approach was used to synthesize titanium dioxide nanotubes. Diverse techniques of characterization were used to evaluate TNTs. The results gained from field emission scanning electron microscopy (FESEM), energy dispersion spectroscopy (EDS), and X-ray diffraction (XRD) indicate that TiO₂ was formed. Gas sensors were created, and the gas detection characteristics were directed towards hydrogen sulfide (H₂S), which is not a healthy gas. The sensor made from these nanotubes responds well to this gas at different temperatures and has high sensitivity. The H₂S-detecting characteristics were evaluated at values ranging from room temperature up to 300 °C. Results show that the gas sensor TNTs that was prepared at 30 volt for H₂S gas sensing has the highest sensitivity and shortest response time at room temperature.

Keywords: Electrochemical deposition, TiO₂ Nanotubes, Hydrogen Sulfide (H₂S), Gas Sensing, Sensitivity

تأثير الفولتية على اداء مستشعر الغاز لصفائف الانابيب النانوية (TiO₂) المحضرة بالانودة

مينا محمد فارس¹ , اسماء كاظم عيال^{2*}

¹ جامعة بغداد , كلية العلوم , قسم الكيمياء

² جامعة بغداد , كلية العلوم للبنات , قسم الكيمياء

الخلاصة

ترتبط الغازات الخطيرة ارتباطاً وثيقاً بالتأثير على حياة الإنسان في البيئة. إن تطور مستشعرات الغاز من خلال الاستجابة العالية له أهمية كبيرة في اكتشاف الغازات الخطرة المختلفة. تعتبر الأنابيب النانوية (TNTs) لثاني أكسيد التيتانيوم (TiO₂) مفضلة في تطبيقات مستشعرات الغاز لما تمتلكه من إمكانات كبيرة وأداء ممتاز. في هذا العمل ، درسنا تأثير الجهد لتحضير انابيب TiO₂ النانوية عبر تقنية الأنودة في تطبيقات استشعار الغاز. تم استخدام طريقة بسيطة من الأنودة الكهروكيميائية لتصنيع الأنابيب النانوية لثاني أكسيد التيتانيوم. تم استخدام تقنيات توصيف متنوعة لتقييم TNTs. تشير النتائج المستحصلة من المجهر الإلكتروني الماسح

*Email: asmaakaa_chem@cs.w.uobaghdad.edu.iq

(FESEM) ، والتحليل الطيفي لتشتت الطاقة (EDS)، وانحراف الأشعة السينية (XRD) إلى أن TiO_2 قد تتشكل. تم إنشاء مستشعرات الغاز و توجيه خصائص الكشف عن الغاز نحو كبريتيد الهيدروجين (H_2S)، وهو غاز ضار بالصحة. يستجيب المستشعر المصنع من هذه الأنابيب النانوية جيدًا لهذا الغاز عند درجات حرارة مختلفة ولديه حساسية عالية. تم تقييم خصائص الكشف عن H_2S بدرجات حرارة تتراوح من درجة حرارة الغرفة إلى $300\text{ }^\circ\text{C}$. أظهرت النتائج أن مستشعر الغاز TNTs المحضر عند $30\text{ }^\circ\text{C}$ فولت لاستشعار غاز H_2S هي أعلى حساسية وأقصر وقت استجابة في درجة حرارة الغرفة.

1. Introduction

With the prompt development of industrialization and the social economy, a considerable amount of industrial waste gases, such as hydrogen sulfide (H_2S), carbon monoxide (CO), nitrogen oxides (NO_x), sulfur dioxide (SO_2), and several volatile organic compounds, are released into the environment. One of the more worrisome pollutants, H_2S , is often found in the production of paper and pulp, coal mining, and natural gas extraction [1-4]. In addition to being corrosive, fetid, poisonous, and combustible, H_2S also affects human breathing, eyes, and the central nervous system at low doses [5,6]. So, it is of significance to improve quite sensitive, reliable, and rapid H_2S sensors. Semiconductors are perfect materials for gas sensors; accordingly, their conductivity is based on the concentration of the gas in contact. Currently, semiconductors of metal oxides such as zinc oxide (ZnO), stannic oxide (SnO_2), indium oxide (In_2O_3), and titanium dioxide (TiO_2) have been utilized to reveal harmful gases [7-12]. TiO_2 is highly applied as a material for gas sensing in order to detect harmful and toxic gases due to its excellent physicochemical properties. Firstly, TiO_2 is an n-type semiconductor with a bandgap of about 3.2 eV [13-17]. Moreover, TiO_2 has the features of chemical stability, environmental friendliness, biocompatibility, and low synthesis cost [18-23]. Secondly, in overview, sensors founded on semiconductors of metal oxide are types that control surface resistance because of the chemisorption of gases on the surfaces of semiconductors. In the reaction, the increased charge carriers on semiconductor surfaces will reduce the thickness of the depletion layer there, which will subsequently cause the resistance of the semiconductor to drop [24]. Importantly, the major interest is in discovering options for operating sensors at low temperatures (room temperature) without losing elevated sensing capacity [25,26]. Nonetheless, the sensitivities of their gas are frequently only obtained at high temperatures, resulting in low durability and high energy consumption [27]. In order to have a large surface area for gas arrival from the surroundings, the size-specific geometrical properties of the structures should exist in the nanodomain to solve this issue. The most encouraging structures are therefore those that are 1D or 2D, such as nanorods, nanotubes, nanobelts, and nanoplates [28,29]. Through these structures, titanium dioxide nanotube arrays have an elevated potential [30]. Therefore, this research aims to study the effect of voltage on preparing TNTs by an anodization method and fabricating them for H_2S sensing. TNTs displayed well-sensing performance at room temperature; thus, these findings lead to increased durability and low-energy consumption.

2. Experimental

2.1. Materials

AnalaR Chemical Company supplied ethylene glycol (EG, 99.5%) and ammonium fluoride (NH_4F , 98.0%). Titanium foils with a thickness of 0.8 mm and a purity of 99.99% were used (Flow Serve Company, USA). In addition, deionized water (DI) (Nanopure Water System, 18 $\text{M}\Omega\text{cm}$ at $25\text{ }^\circ\text{C}$) was used to produce all the solutions during the experiment. A power supply (Laboratory DC Power Supply, TM-605) was employed as the voltage source.

2.2. Synthesis of TNTs nanofilm

In this study, the electrochemical anodization procedure was used to prepare TNTs [31]. Firstly, the Ti foil was ultrasonically cleaned for 15 minutes with acetone, followed by 15 minutes each with ethanol and DI water before anodization, and then etched with 6 M HNO₃ before anodization. Anodization of TNTs on Ti foil (10 mm × 20 mm × 0.8 mm) was applied in a cell with two electrodes. Titanium foil was the working electrode, while graphite was the counter electrode (a 2 cm distance between the electrodes was maintained). NH₄F (0.5 wt%) dissolved in water (5 vol%) with ethylene glycol as the electrolyte. The cell was attached to a power supply and subjected to different voltages (10, 20, 30, and 40 volts) for 1 hour at room temperature. After that, the prepared samples were washed with DI water. To obtain TNTs, the prepared samples were annealed at 500 °C for one hour at a rate of heating of 2 °C.min⁻¹.

2.3. Characterization of TNTs

The morphologies of TNT nanofilm were studied using a field emission scanning electron microscope (FESEM) (MERLIN, ZEISS, Germany), while element analysis was done using energy dispersive X-ray (EDS) spectrometers. Then, using Cu K α radiation ($\lambda = 0.1541$ nm) in X-ray with voltage (60 kV) and current (60 mA), X-ray diffractometry (X-ray, PANALYTICAL, X-Pert Pro) was used to identify the phase composition of TNT samples. Moreover, the data on patterns were gathered with 2 theta, ranging from 10 to 80 °C. The crystallite sizes (D) of TNTs were calculated using the Scherrer equation [32].

$$D = \frac{0.89 \lambda}{\beta \cos \theta} \quad (1)$$

where λ is the wavelength of the X-rays, $\cos \theta$ and β are the incident angles of the X-rays, and the full width is half the maximum of the maximum diffraction peak, respectively.

2.4. Measurements of gas sensing

A suitable setup is created with the intention of determining the sensitivity parameter, which mostly pertains to the reaction time and recovery time of the manufactured TiO₂ gas sensor detector. The schematic design shows how the test setup functions (Figure 1). The sensor was first put on the heater after the test chamber was opened. The conductive aluminum sheet was used to make the appropriate electrical connections between the pin feedthrough and the sensor, and then the test chamber was sealed. After that, a bias voltage of 6 volts was supplied across the electrodes' two sides. The test chamber was then evacuated to a pressure of around 1 mbar using the rotary pump, and the sensor's working temperature was then adjusted using a temperature controller. The needle valves were used to control the H₂S gas flow rate, and the PC-interfaced digital multimeter of type UNI-UT81B was used to monitor the current fluctuation. First, the biasing current of air flow was recorded by the digital multimeter; after that, the testing gas (H₂S) was switched on, and after several seconds the current had low variation; then the test gas was switched off to record the recovery time.

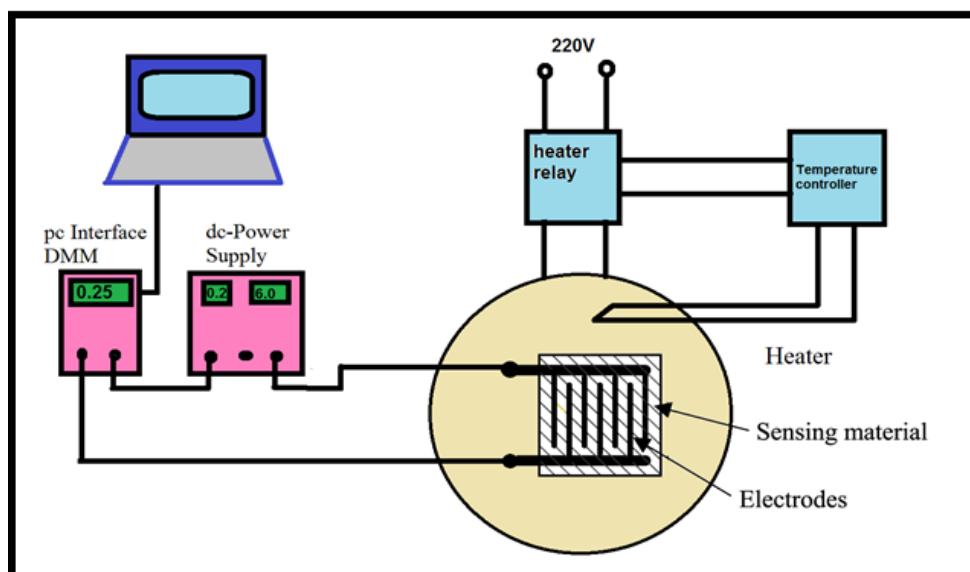


Figure 1 : Schematic diagram of gas sensing and the electrical circuit setup

The gas sensor's reaction and recovery times (TNTs) describe how long is needed for the response to increase to 90% of the stable value and decrease to 10% of its superior value after adding and removing gas, respectively. Furthermore, the sensor's sensitivity can be calculated using equation 2 [33-35]:

$$S\% = \frac{R_{on} - R_{off}}{R_{off}} \times 100\% \quad (2)$$

where S is the sensitivity of the sensor, while R_{on} , and R_{off} are the electrical resistances of the sensor in the gas and air, respectively.

3. Result and discussion

3.1. Structural and morphological characteristics

Figure 2a-d display the FESEM images of TNTs that were prepared at different voltages (10, 20, 30, and 40 volts). As shown in Figure 2, the TNTs became clearer and the nanotubes grew longer as the voltage increased. The improvement in the diameter and length of the tubes can be noted by adjusting the voltages of anodization [36,37]. Figure 2a shows that the TiO_2 nanotubes have not been formed under this oxidation voltage (10 volts). TNTs were formed, however, when the voltage was increased to 20 and higher. It is recognized from the mechanism of the reaction that the growth phase of the TNTs has entered. However, the top view and cross-section of TNTs nanotubes formed at various voltages are shown in Figure 2. The inner and outer diameters of TiO_2 nanotubes, as well as their lengths, may be calculated from photographs. Under anodization conditions, the inner and outer diameters of TiO_2 nanotubes are 53 to 133 nm and 65 to 150 nm, respectively, and the tube length is 1.8 to 5.87 μm .

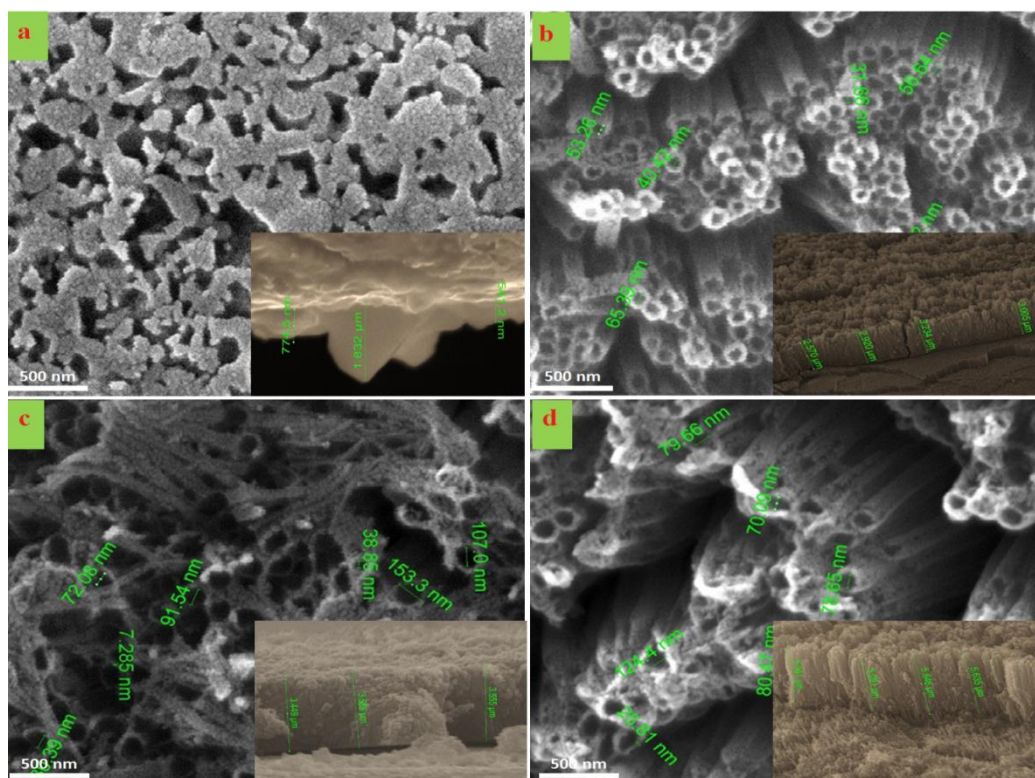


Figure 2: Top view FESEM images of TNTs prepared at: (a) 10 V ; (b) 20 V; (c) 30 V, and (d) 40 V). Cross-sectionals of the TNTs are displayed in the inset of the figure

EDS was also used to analyze the elements of TNTs that were prepared at different anodization voltages. The elemental weight percentages of TNTs were mentioned as given in Table 1. In addition, Figures 3 and 4 display the EDS spectrum and elemental mapping of TNTs that confirm the presence of titanium and oxygen elements. Furthermore, fluorine and carbon come from the electrolyte of anodizing. While at 10 volt, iron was detected, which was confirmed to come from the composition of the titanium foil. Thus, it proved that 10 volt was not a suitable voltage to prepare TNTs with high purity.

Table 1 : EDS analysis for TNTs at at different voltages (10, 20, 30, and 40 volts)

Applied voltage (volt)	Element	Weight (%)	Weight (% Error)
10	C	5.4	0.1
	N	3.7	0.2
	O	19.4	1.0
	Ti	71.3	0.2
	Fe	0.2	0.0
20	C	4.8	0.1
	N	3.4	0.3
	O	22.6	2.4
	Ti	69.2	0.2
30	C	4.6	0.1
	N	3.0	0.3
	O	21.1	1.9
	Ti	71.3	0.2
40	C	5.3	0.1
	N	3.6	0.5
	O	22.8	3.4
	Ti	68.2	0.3

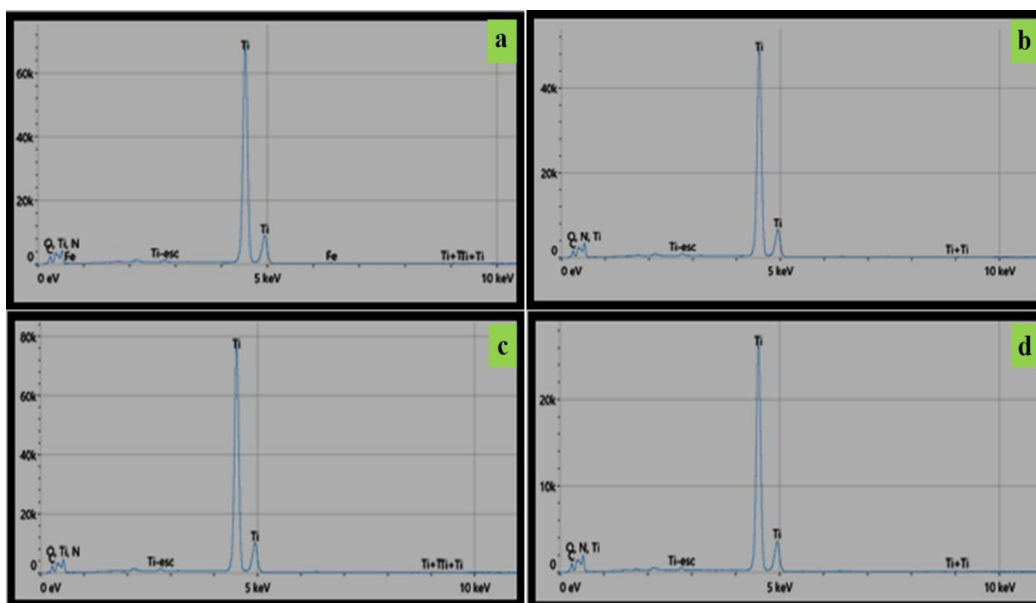


Figure 3 : EDS of TNTs prepared at : (a) 10 V ; (b) 20 V; (c) 30 V, and (d) 40 V

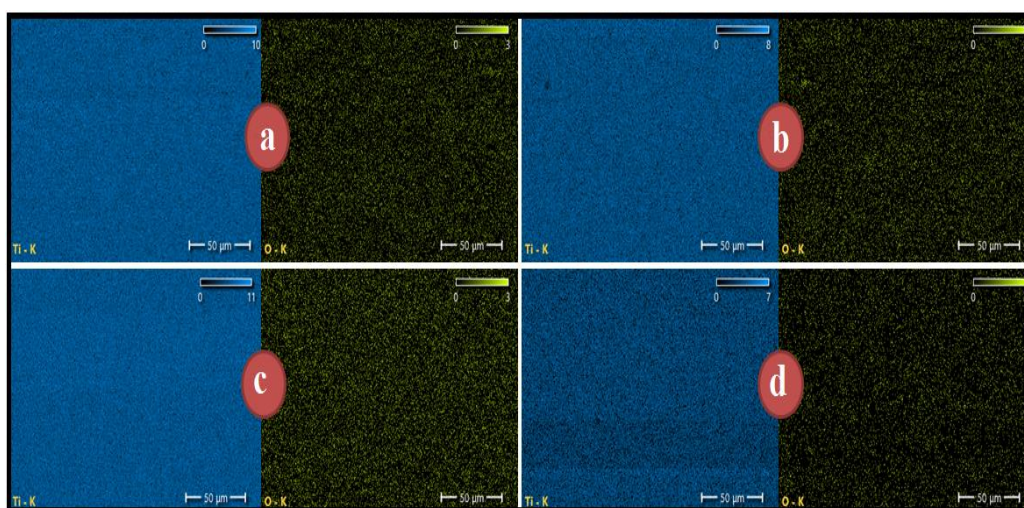


Figure 4 : EDS elemental mapping of TNTs prepared at: (a) 10 V ; (b) 20 V; (c) 30 V, and (d) 40 V

Figure 5 shows the X-ray diffraction patterns of the synthesized samples with different voltages of anodization. Alongside the strong diffraction peaks matching the titanium foil substrate (reference code: 00-051-0631). Six diffraction peaks were detected at 24.93° , 37.67° , 47.93° , 53.78° , 62.11° , and 75.08° were also located in all the prepared samples. The peaks of diffraction are listed in the lattice planes 101, 004, 200, 105, 213, and 215 according to reference code 00-021-1272. Thus, we deduced that TiO_2 (anatase) was formed on the titanium foil mesh's surface. Besides, one-diffraction peak corresponds to the rutile TiO_2 according to the reference code 00-021-1276. According to the XRD examination, the TNTS nanotubes are polycrystalline, and using the data from the XRD in Figure 5, the average crystallite size (14.9 nm) from the total width at half the maximum of TiO_2 anatase 101 diffraction peaks is calculated using Equation 1.

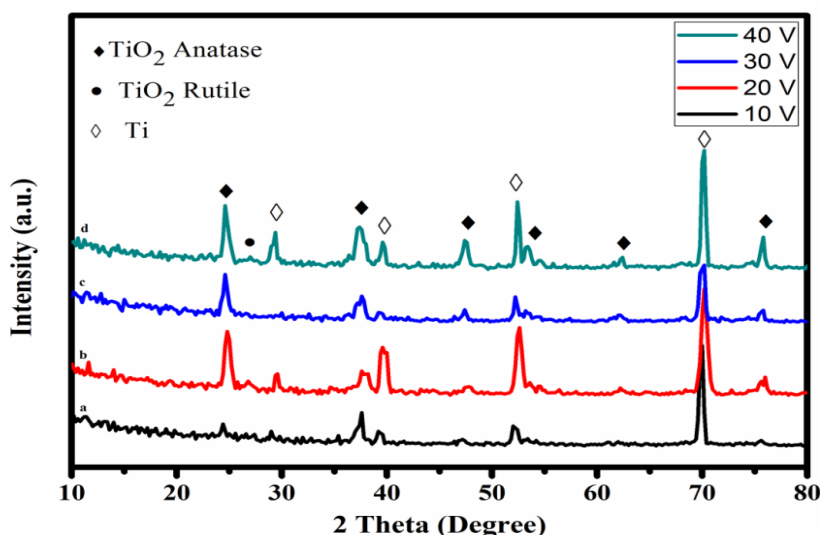


Figure 5 : XRD diffractograms of TNTs prepared at different voltages (10, 20, 30, and 40 volts)

3.2. Performance of gas sensing

The variations in the resistance of semiconductors are the foundation for the sensing efficiency of semiconductors. These variations are caused by the interactions between atmospheric gases and semiconductors. In order to characterize the features of gas sensing, dynamic alterations in resistance are used. The ratio of the resistance in air to the resistance when the gas is present (R_a/R_g) is commonly used to describe the sensitivity response of the gas sensor, an n-type semiconductor, to a reducing gas. In contrast, the response of an oxidizing gas is described as the resistance of the gas to resistance without the presence of the gas (R_g/R_a) [34]. The results of the interference between gas and TiO₂ nanotubes showed that when the H₂S gas was introduced, the resistance of the TiO₂ nanotube sensor decreased. Figures 6-9 shows a typical response of the n-type gas sensor (TiO₂ nanotubes) to the reducing gas (H₂S), which was confirmed by the resistance in the air being greater than the resistance in the presence of the gas [38].

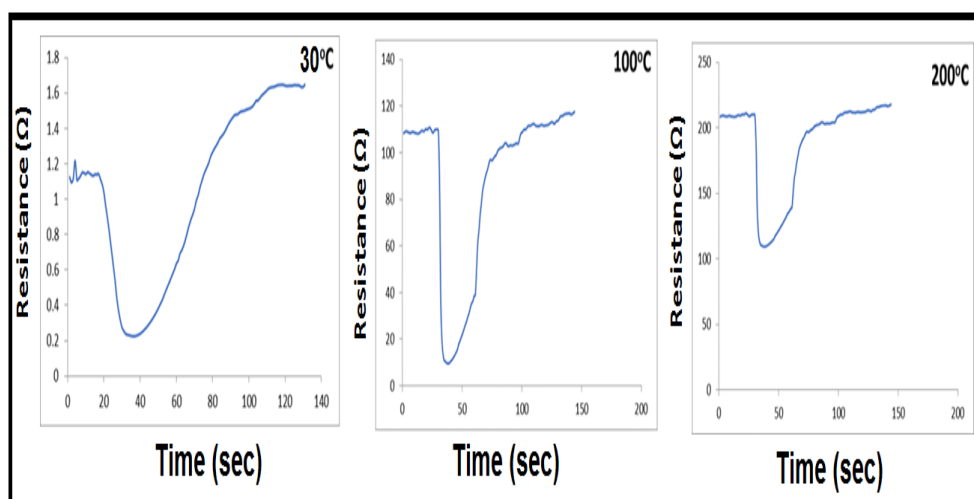


Figure 6 : Change in the resistance of TNTs prepared at 10 volt to H₂S gas at different operating temperatures

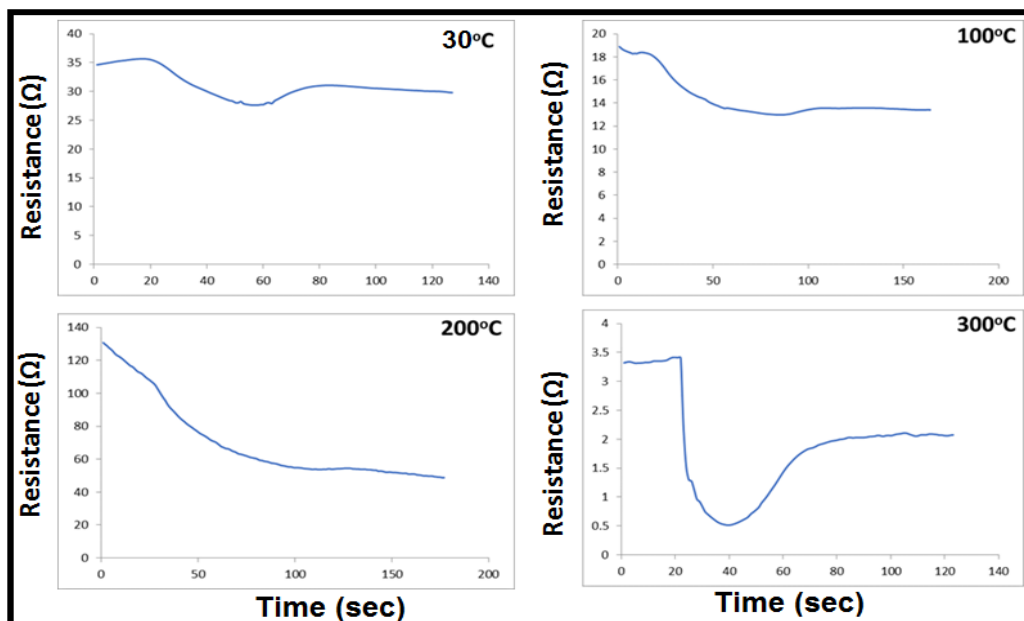


Figure 7 : Change in the resistance of TNTs prepared at 20 volt to H₂S gas at different operating temperatures

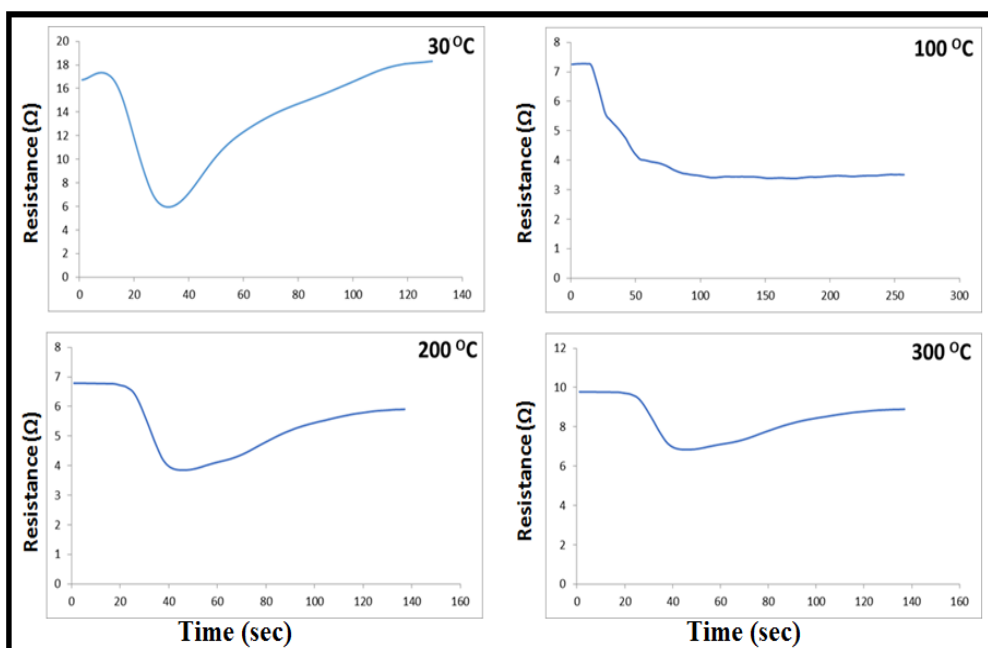


Figure 8 : Change in the resistance of TNTs prepared at 30 volt to H₂S gas at different operating temperatures

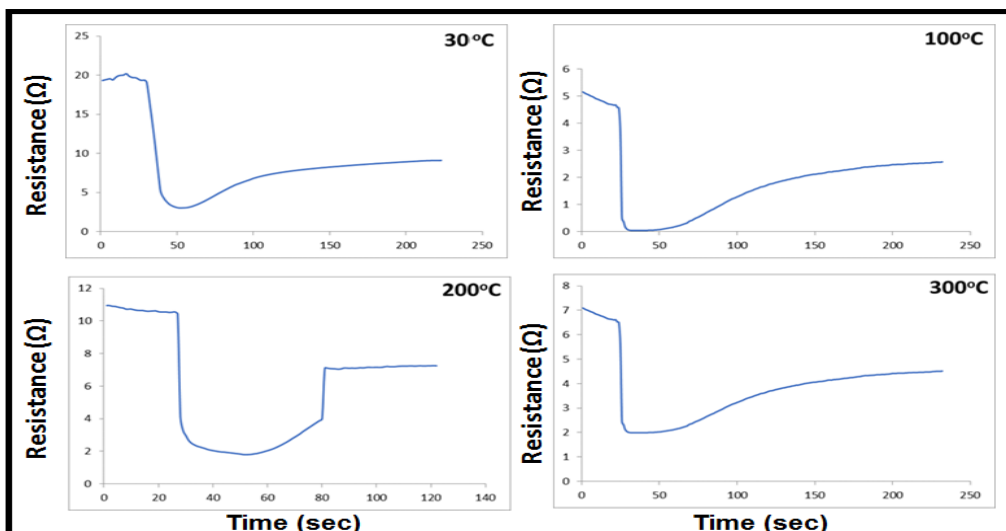


Figure 9 : Change in the resistance of TNTs prepared at 40 volt to H₂S gas at different operating temperatures

Response and recovery times are the primary concerns for gas sensing properties, particularly at low operating temperatures. To select the optimal temperature for the working of the prepared TNTs gas sensor at different anodizing voltages, the gas sensors' responses to 450 ppm H₂S were examined at an operating temperature starting from room temperature up to 300 °C, as shown in Figure 10. According to Figure 10, the response times of H₂S gases *via* the TNTs that were prepared at 30 volt were less compared to the TNTs sensors that were prepared at 10, 20, and 40 volts. Furthermore, at the operating temperature (room temperature), all the prepared samples as gas sensors appeared to have a good response time for H₂S sensing of less than 28 seconds. While the recovery times of all gas sensors prepared at 10, 20, 30, and 40 volts at a lower working temperature were 72.9, 58.5, 155.7, and 138.6 seconds, respectively. TNTs at 30 volt could be the perfect nanostructure for gas detection due to their ingrained qualities of a considerable surface area, superior rate of electron transport, intense adsorption capacity [39], and many porous positions for the prompter diffusion of the gas [40,41].

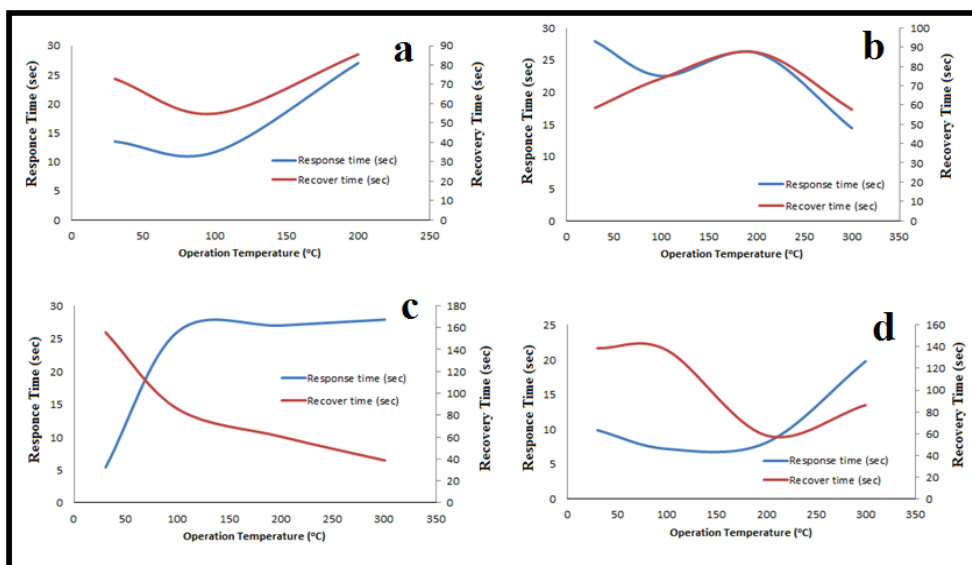


Figure 10 : Response and recovery times of TNTs prepared at : (a) 10 V (b) 20 V, (c) 30 V, and (d) 40 V

Figure 11 shows the gas sensitivity of the TNTs sensor to H_2S at different operating temperatures ranging from room temperature to $300\text{ }^\circ\text{C}$ at a 450 ppm concentration of H_2S . The sensitivity of TNTs sensors ranged from about 4.365 to 38.107% , and the highest sensitivity at room temperature was 38.107% for the TNTs sensor that was prepared at 30 volt . That way proves that the sensing sensitivity is mostly changed by different working temperatures. The highest sensitivity at room temperature for TNTs sensor was caused by the high porosity and large diameter of TNTs thin film, which allowed for easy adsorption and desorption of gas molecules [42].

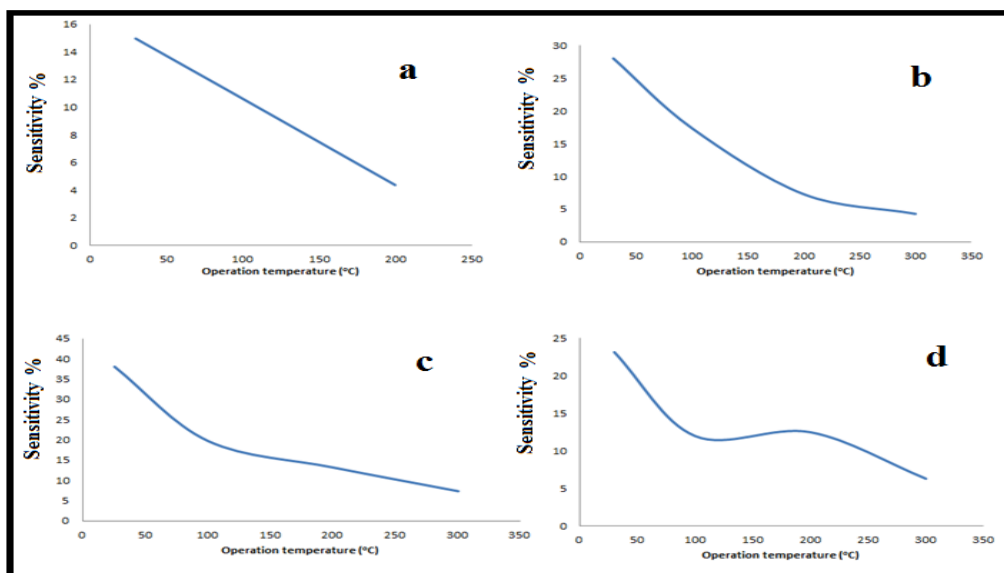


Figure 11 : Sensitivity of TNTs prepared at (a) 10 V (b) 20 V , (c) 30 V , and (d) 40 V

The sensing mechanism of TNTs gas sensors generally depends on the surface characteristics of the nanomaterial. Firstly, the adsorption of oxygen from the atmosphere takes place. The adsorbed oxygen elicits the electrons of the conduction band from the surface of TNTs grains, leaving behind positively charged donor ions. The electrical field between negatively charged oxygen ions such as O^- or O^{2-} and positively charged donor ions become stronger. As a result, the greater the number of oxygen ions on the surface, the greater the potential barrier, and thus the greater the resistance. Because of the reaction with gas molecules, the amount of O^- or O^{2-} in the environment decreases as the gas is present, resulting in a decrease in resistance [43]. So, At room temperature, the TNTs gas sensor has an unusually good response. This is most likely due to the fact that TiO_2 nanotubes are made up of tiny nanocrystals that have been linked together into a 1D tubular shape. As a result, there are a lot of active sites for gas chemisorption. The walls of TiO_2 nanotubes may also be able to hold a lot of gas molecules, so the nanotubes can act as gas diffusion nanochannels [44].

4. Conclusion

The anodization technique was applied to prepare highly ordered TiO_2 nanotube arrays (TNTs). Furthermore, this work focused on the influence of voltages on the surface characteristics of TNTs and then the effect on the TNTs as a gas sensor. Results of the test of gas sensing show that TNTs at 30 volt achieved a significantly greater sensitivity to H_2S at room temperature as well as a shorter response time. The superb efficiency of the TNTs in gas detection may be attributed mostly to their extremely ordered nanotube morphology and their high surface area. This study provides the possibility of studying the sensing of H_2S *via* observation of the response and recovery time at the different operating temperatures of H_2S gas at a constant concentration of 450 ppm . Thus, this study demonstrated the possibility to

improve the TNTs sensor for the detection of H₂S gas at low temperatures (room temperature) with high sensitivity, which, compared with the flammable H₂S gas, can be more helpful for the production of H₂S gas sensors.

Acknowledgments

Special thanks are extended to the Chemistry Department, College of Science for Women, and the University of Baghdad, Baghdad, Iraq.

Conflict of interest

The authors declare that they have no known personal relationships or financial interests that could have been shown to affect the study reported in this paper.

References

- [1] A. A. Jameh, T. Mohammadi, O. Bakhtiari, and M. Mahdiyfar, "Synthesis and modification of zeolitic imidazolate framework (ZIF-8) nanoparticles as highly efficient adsorbent for H₂S and CO₂ removal from natural gas", *The Journal of Environmental Chemical Engineering*, vol. 7, no. 3, p. 103058, 2019.
- [2] X. Tong, W. Shen, X. Chen, and J. Corriou, "Qualitative and quantitative analysis of gaseous pollutants for cleaner production in pulp and paper mills", *The Journal of Cleaner Production*, vol. 198, pp. 1066-1075, 2018.
- [3] Q. Deng, J. Yin, X. Wu, T. Zhang, H. Wang, and M. Liu, "Research advances of prevention and control of hydrogen sulfide in coal mines", *Hindawi*, vol. 2019, no. 1975, pp. 1-16, 2019.
- [4] X. Tong, W. Shen, X. Zhang, J. Corriou, and H. Xi, "Synthesis and density functional theory study of free-standing Fe-doped TiO₂ nanotube array film for H₂S gas sensing properties at low temperature", *Journal of Alloys and Compounds*, vol. 832, no. 2, pp. 155015-155026, 2020.
- [5] Y. Lei, K. Wang, S. Chen, Q. Zhang, and Z. Hu, "A fluorescent probe based on tetrahydro[5]helicene for highly selective recognition of hydrogen sulfide", *Spectrochimica Acta Part A: Molecular and Biomolecular Spectroscopy*, vol. 204, pp. 295-300, 2018.
- [6] S. Panthi, S. Manandhar, and K. Gautam, "Hydrogen sulfide, nitric oxide, and neurodegenerative disorders", *Translational Neurodegeneration*, vol. 7, no. 3, pp. 1-8, 2018.
- [7] G. Korotcenkov and B. K. Cho, "Metal oxide composites in conductometric gas sensors: achievements and challenges", *Sensors and Actuators B: Chemical*, vol. 244, pp. 182-210, 2017.
- [8] T. Lin, X. Lv, Z. Hu, A. Xu, and C. Feng, "Semiconductor metal oxides as chemoresistive sensors for detecting volatile organic compounds", *Sensors*, vol. 19, no. 2, pp. 233-234, 2019.
- [9] A. Mirzaei, S. S. Kim, and H. W. Kim, "Resistance-based H₂S gas sensors using metal oxide nanostructures: A review of recent advances", *Journal of Hazardous Materials*, vol. 375, no. 5, pp. 314-331, 2018.
- [10] J. Bai and B. Zhou, "Titanium dioxide nanomaterials for sensor applications", *Chemical Reviews*, vol. 114, no. 19, pp. 10131-10176, 2014.
- [11] M. A. Raza, A. Habib, Z. Kanwal, S. S. Hussain, M. J. Iqbal, M. Saleem, S. Riaz, and S. Naseem, "Optical CO₂ gas sensing based on TiO₂ thin films of diverse thickness decorated with silver nanoparticles", *Hindawi*, vol. 2018, pp. 1-12, 2018.
- [12] R. S. Khaleel and M. S. Hashim, "Fabrication of TiO₂ sensor using rapid breakdown anodization method to measure pressure, humidity and sense gases at room temperature", *Iraqi Journal of Science*, vol. 60, no. 8, pp. 1694-1703, 2019.
- [13] B. Viswanathan, "Fabrication and characterization of uniform TiO₂ nanotube arrays by sol-gel template method", *Bulletin of Materials Science*, vol. 29, no. 7, pp. 705-708, 2006.
- [14] A. Kadim, Z. Zainal, A. Mebdir, H. Lim, Z. Abidin, and Y. Lim, "Journal of Physics and Chemistry of Solids Sensitization of TiO₂ nanotube arrays photoelectrode via homogeneous distribution of CdSe nanoparticles by electrodeposition techniques", *The Journal of Physical Chemistry*, vol. 153, no. 2, pp. 110006, 2021.
- [15] M. Mollavali, S. Rohani, and M. Elahifard, "Science direct band gap reduction of (Mo p N) co-doped TiO₂ nanotube arrays with a significant enhancement in visible light photo-conversion: A combination of experimental and theoretical study", *International Journal of Hydrogen Energy*, vol. 46, no. 41, pp. 21475-21498, 2021.

- [16] M. A. Henderson, "A surface science perspective on TiO₂ photocatalysis", *Surface Science Reports*, vol. 66, pp. 185-297, 2011.
- [17] T. J. Awaid, A. K. Ayal, A. M. Farhan, and L. Y. Chin, "Effect of electrolyte composition on structural and photoelectrochemical properties of titanium dioxide nanotube arrays synthesized by anodization technique", *Baghdad Science Journal*, vol. 17, no. 4, pp. 1183-1189, 2020.
- [18] J. Woo, D. Phan, Y. W. Jung, and K. Jeon, "Fast response of hydrogen sensor using palladium nanocube-TiO₂ nanofiber composites", *International Journal of Hydrogen Energy*, vol. 42, no. 29, pp. 18754-18761, 2017.
- [19] A. K. Ayal, "Enhanced photocurrent of titania nanotube photoelectrode decorated with CdS nanoparticles", *Baghdad Science Journal*, vol. 15, no. 1, pp. 57-62, 2018.
- [20] L. M. Anaya-Esparza, Z. Villagrán-de la Mora, J. M. Ruvalcaba-Gómez, R. Romero-Toledo, and T. Sandoval-Contreras, S. Aguilera-Aguirre, E. Montalvo-González, and A. Pérez-Larios, "Use of titanium dioxide (TiO₂) nanoparticles as reinforcement agent of polysaccharide-based materials", *Processes*, vol. 8, no. 11, pp. 1-26, 2020.
- [21] N. A. Samsudin, Z. Zainal, H. N. Lim, Y. Sulaiman, S. K. Chang, Y. C. Lim, A. K. Ayal, and W. N. M. Amin, "Capacitive performance of vertically aligned reduced titania nanotubes coated with Mn₂O₃ by reverse pulse electrodeposition", *RSC advances*, vol. 8, no. 41, pp. 23040-23047, 2018.
- [22] K. Lingaraju, R. B. Basavaraj, K. Jayanna, S. Bhavana, S. Devaraja, H. M. Kumar Swamy, G. Nagaraju, H. Nagabhushana, and H. R. Naika, "Biocompatible fabrication of TiO₂ nanoparticles: Antimicrobial, anticoagulant, antiplatelet, direct hemolytic and cytotoxicity properties", *Inorganic Chemistry Communications*, vol. 127, no. August 2020, p. 108505, 2021.
- [23] A. M. A. Al-Sammarráie, H. I. Jaafer, and H. H. Hamdan, "Study of the effect of NH₄F concentration on the structure of electrochemically prepared TiO₂ nanotubes", *Iraqi Journal. Science.*, vol. 53, no. 2, pp. 827-831, 2012.
- [24] D. A. Zimnyakov, M. Y. Vasilkov, and S. A. Yuvchenko, "Light-Tuned DC Conductance of Anatase TiO₂ Nanotubular Arrays : Features of Long-Range Charge Transport", *Nanomaterials*, vol. 8, no. 915, pp. 1-17, 2018.
- [25] T. Plecenik, M. Moško, A. A. Haidry, P. Ďurina, M. Truchlý, B. Grančič, M. Gregor, T. Roch, L. Satrapinskyy, A. Mošková, and M. Mikula, "Fast highly-sensitive room-temperature semiconductor gas sensor based on the nanoscale Pt-TiO₂-Pt sandwich", *Sensors and Actuators B: Chemical.*, vol. 207, no. Part A, pp. 351-361, 2015.
- [26] A. S. Varezchnikov, F. S. Fedorov, I. N. Burmistrov, I. A. Plugin, M. Sommer, A. V. Lashkov, A. V. Gorokhovskiy, A. G. Nasibulin, D. V. Kuznetsov, M. V. Gorshenkov, and V. Sysoev, "The room-temperature chemiresistive properties of potassium titanate whiskers versus organic vapors", *Nanomaterials*, vol. 7, no. 455, pp. 1-11, 2017.
- [27] K. Arshak, E. Moore, G. M. Lyons, J. Harris, and S. Clifford, "Sensor review emerald article : A review of gas sensors employed in electronic nose applications A review of gas sensors employed in electronic nose applications", *Sensor Review*, vol. 24, no. 2, pp. 181-198, 2004.
- [28] J. Huang and Q. Wan, "Gas sensors based on semiconducting metal oxide one-dimensional nanostructures", *Sensors*, vol. 9, pp. 9903-9924, 2009.
- [29] X. Liu, T. Ma, N. Pinna, and J. Zhang, "Two-dimensional nanostructured materials for gas sensing", *Advanced Functional Materials*, vol. 27, no. 37, p. (1702168) 1-30, 2017.
- [30] E. Comini, V. Galstyan, G. Faglia, E. Bontempi, and G. Sberveglieri, "Highly conductive titanium oxide nanotubes chemical sensors", *Microporous Mesoporous Materials*, vol. 208, pp. 165-170, 2015.
- [31] A. Kadim, A. Ayat, K. Hashim, A. Mudhafar, M. Ahlam, and M. Farhan, "Electrochemical deposition of Cu-nanoparticle-loaded CdSe/TiO₂ nanotube nanostructure as photoelectrode", *Journal of Electronic Materials*, vol. 50, no. 9, pp. 5161-5167, 2021.
- [32] A. M. Holi, A. K. Ayal, and A. A. Baqer, "Construction of ZnO-nanoflowers photoanode for photoelectrochemical cell", *Journal of Physics: Conference Series*, vol. 1234, pp. 1-10, 2019.
- [33] I. H. Kadhim, H. A. Hassan, and F. T. Ibrahim, "Hydrogen gas sensing based on nanocrystalline SnO₂ thin films operating at low temperatures", *International Journal of Hydrogen Energy*, vol. 45, no. 46, pp. 25599-25607, 2020.
- [34] Q. Qin and D. Olimov, "Semiconductor-type gas sensors based on γ -Fe₂O₃ nanoparticles and its derivatives in conjunction with SnO₂ and graphene", *Chemosensors*, vol. 10, no. 7, pp. 267-278,

- 2022.
- [35] S. B. Deshmukh and R. H. Bari, "Nanostructured ZrO₂ thin films deposited by spray pyrolysis techniques for ammonia gas sensing application", *International Letters of Chemistry, Physics and Astronomy*, vol. 56, no. 2, pp. 120-130, 2015.
- [36] A. K. Ayal, "Effect of anodization duration in the TiO₂ nanotubes formation on Ti foil and photoelectrochemical properties of TiO₂ nanotubes", *Al-Mustansiriyah Journal Science*, vol. 29, no. 3, pp. 77-81, 2018.
- [37] H. Li, G. Wang, J. Niu, E. Wang, G. Niu, and C. Xie, "Results in physics preparation of TiO₂ nanotube arrays with efficient photocatalytic performance and super-hydrophilic properties utilizing anodized voltage method", *Results Physics*, vol. 14, p. 102499, 2019.
- [38] T. A. Vincent and J. W. Gardner, "H₂S sensing properties of WO₃ based gas sensor", *Procedia Engineering*, vol. 168, pp. 255-258, 2016.
- [39] K. Lee, R. Kirchgeorg, and P. Schmuki, "Role of transparent electrodes for high efficiency TiO₂ nanotube based dye-sensitized solar cells", *Journal Physics Chemistry C*, vol. 118, no. 30, pp. 16562-16566, 2014.
- [40] P. Bindra, S. Member, S. Gangopadhyay, and A. Hazra, "1-D TiO₂ nanorods array based parallel electrode sensor for selective and stable detection of organic vapors", *IEEE Sensors Journal*, vol. PP, no. iii, pp. 1-8, 2019.
- [41] A. M. Holi, G. A. Al-Sajad, A. A. Al-Zahrani, and A. S. Najm, "Nano biomed eng enhancement in NO₂ and H₂-sensing performance of Cu_xO/TiO₂ nanotubes arrays sensors prepared by electrodeposition synthesis", *Nano Biomed Engineering*, vol. 14, no. 2, pp. 7-14, 2022.
- [42] A. M. Serventi, D. G. Rickerby, M. C. Horrillo, and R. G. Saint-jacques, "Transmission electron microscopy investigation of the effect of deposition conditions and a platinum layer in gas-sensitive r.f.-sputtered SnO₂ films", *Thin Solid Films*, vol. 445, pp. 38-47, 2003.
- [43] P. R. Padole, "Characterization of nanosized TiO₂ based H₂S gas sensor", *Journal Mater Science*, vol. 41, pp. 4860-4864, 2006.
- [44] X. Xiao, K. Ouyang, R. Liu, and J. Liang, "Anatase type titania nanotube arrays direct fabricated by anodization without annealing", *Applied Surfaces Science*, vol. 255, pp. 3659-3663, 2009.